Feasibility of LDM to Serve User-IoT Pairs in Future Cellular Network

Md Shantanu Islam, Raouf Abozariba, A. Taufiq Asyhari, Mohammad Patwary, and Mohammad A Matin

Abstract. The future wireless network aims to accommodate new forms of services arising from the large scale inclusion of the internet of things (IoT). This inclusion of IoT and ever-increasing users will require the future network to possess higher system capacity and manage heterogeneity in the service requirement. Layer division multiplexing (LDM) is a potential technology that can enhance network capacity by taking advantage of this inherent heterogeneity of future wireless networks. This chapter presents a transmission framework where the LDM layer serves IoT-user pairs. The IoT devices are served using an LDM upper layer (UL), and the users are served using a lower layer (LL). We have developed a physical layer model incorporating LDM and tested its performance for the intended usages scenario. Both UL and LL performance show the capability to serve IoT devices and users to justify our proposed transmission scenario. Mobility management for LDM LL is a crucial challenge as it was initially developed for static receivers. Moreover, the mobility of both IoT devices and the user impacts the LDM pair sustainability. To test our system's robustness against receiver mobility, we have developed an analytical model to test the link sustainability for LDM pairs when both receivers have different levels of mobility. We have also included massive multiple-input multiple-output transmission and beamforming in the system model, focusing on the future wireless network. For simulation, We have considered three different mobility models for both types of receivers, and link sustainability for LDM pairs belonging to different mobility groups are compared to determine the more suitable LDM pair from receiver mobility. The achieved results show that LDM can enhance the system capacity in future wireless networks.

Keywords: LDM, NOMA, B5G, Receiver-Mobility, Sustainable link time

Md Shantanu Islam, Raouf Abozariba and A. Taufiq Asyhari
School of Computing and Digital Technology, Birmingham City University, United Kingdom

Mohammad Patwary
Department of Computer Science, University of Wolverhampton, United Kingdom

Mohammad A Matin
Department of Electrical and Computer Engineering, North South University, Dhaka, Bangladesh

1 Introduction

The future wireless system's development is focused on achieving higher capacity and flexibility than the existing systems. The future network should provide seamless services to new types of services such as the internet of things (IoT), enhanced Mobile BroadBand (eMBB) communications and tactile internet. These services are setting the standards for the long term evolution of fifth-generation (5G) and beyond 5G (B5G) [1]. Multiple technologies have the potential to achieve this seamless connectivity with increased user capacity. Non-orthogonal multiple access (NOMA) is one such potential technology [2, 3].

In this chapter we are exploring the application and feasibility of LDM in future wireless communication to achieve higher network capacity while delivering the required standard of user and IoT communications. We have developed a reliable downlink transmission framework and usages model that can take advantage of the different characteristics of the LDM layers. LDM is a layer division or power-based NOMA which can be configured with diverse power levels (layers) to provide different services using its Upper and Lower layer [4]. LDM can serve two different services using a single traffic channel (OFDM channel as will be presented later) as both layers can use the available time and frequency slot of the traffic channel simultaneously. This characteristic makes LDM a more spectral efficiency system as it can use the available channel capacity for both layers with intelligent layer configuration. One such simple structure is used in the integration of LDM into advanced television systems committee (ATSC 3.0) PHY layer baseline technology [5]. In this case, a robust configuration is implemented in the Upper (Core) Layer (UL), oriented to portable and mobile receivers. On the other hand, in the Lower (Enhance) Layer (LL), a high capacity configuration is chosen to deliver high data rate services, such as ultra-high-definition television (UHDTV) or multiple high definition television (HDTV) services, to fixed receivers. Motivated from the successful integration of LDM in ATSC 3.0, we have investigated the possibilities of convergence between the user and IoT devices based on their difference in required data rate and network condition. In our model, the UL is used to serve the IoT communications while LL is used to serve the users (e.g. mobile handsets). As the model is developed for future wireless needs, it has to perform with user mobility. We have aimed to implement LDM UL and LL for the mobile user, which is a challenge as in ATSC 3.0, static users are considered LL receivers.

We have developed an OFDM physical layer framework to adopt LDM into our transmission model. In principle, heterogeneity for the 5G network is dictated by QoE/QoS of different applications – in terms of latency, privacy, data rate, accuracy, and robustness requirements. LDM Upper and Lower layers can address these heterogeneous requirements as UL offers higher accuracy and robustness with lower latency; in contrast, LL can ensure better privacy and a higher data rate. In this chapter, we are looking into a downlink transmission scenario for IoT and users. Moreover, the impact of mobility on the formation and termination of IoT pairs will be explained. A way to calculate LDM link sustainability for combining different mobility models of both receivers is developed and explained. This chapter aims to give readers an insight into the LDM's applicability in future wireless communication.

The remainder of the chapter is structured as follows: Key works in LDM for broadcasting and 5G wireless communication is discussed in section 2. The use case scenario of this transmission system is described in section 3. The system model is described for the downlink communication scenario in section 4. An analytical framework for LDM performance evaluation is presented in section 5. The device mobility model and its impact on the LDM pair is discussed in section 6. Section 7 describes our findings and relevant analysis. Moreover, the outcome is summarised in the final section 8.

2 Literature Review

LDM is a power-based NOMA technology that was introduced in cloud transmission (a flexible multi-layer system that uses spectrum overlay technology to deliver multiple program streams simultaneously) [6] in 2012. Later, LDM was accepted for use in the physical layer design of advanced television systems committee (ATSC) 3.0 due to its higher degree of flexibility and performance advantages over existing orthogonal multiple access (OMA) techniques [7]. LDM can combine various services in a single radio frequency (RF) channel to support multiple user applications using the same traffic channel. Since adapting LDM into ATSC 3.0 physical layer design, much work has been done on finding the LDM's performance for the downlink broadcast transmission. Reference [8] for example investigated this performance trade-off between UL and LL where capacity and coverage performance of LL at the cost of that of UL is shown for ATSC 3.0. [8] work shows a better performance of LDM compared with time-division multiplexing (TDM) and frequency-division multiplexing (FDM). Reference [9] proposed a multiple physical layer pipe (M-PLP) configuration based on multi-layer LDM and performed a capacity analysis of this configuration to determine the lower capacity bound (approximately 1 Mbps) of UL. In [10] the authors showed that LDM UL provides higher channel capacity than TDM/FDM at a low signal to noise ratio (SNR), and LL can do the same at high SNR conditions. Due to increased capacity gain over TDM and FDM, LDM is gaining interest in 5G deployment. Many have investigated the possibility of using LDM in point to multipoint (P2MP) and broadcasting transmission in 5G wireless communication. Both [11], [12] investigated the capacity improvement of LDM over OMA techniques for providing multimedia services in 5G and found that LDM offers higher channel capacity. On the other hand, in [13] higher network throughput is achieved by using LDM for a unicast-broadcast convergence. These works show that LDM can serve heterogeneous devices and increase network capacity. Most of the works on LDM are focused on exploiting its advantages for broadcast multimedia transmission; these works motivated us to look for other use cases where LDM can be successful. In our previous work [14], we proposed a system model that uses LDM to take advantage of the heterogeneity requirements of user and IoT devices. Our analysis showed that LDM increased capacity is achieved only

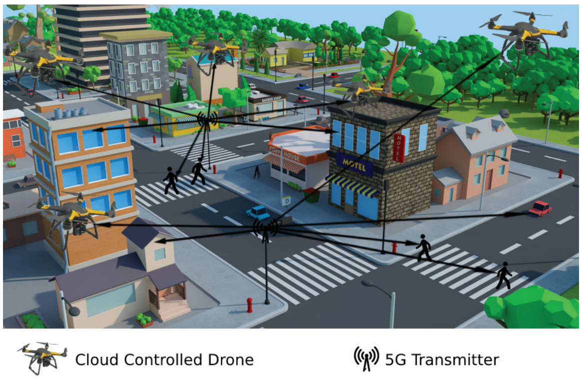

Fig. 1. Downlink transmission model for IoT devices in urban area

at higher SNR for both UL and LL. Due to this higher SNR requirement, the impact of the rapid changes in the channel condition arising from the mobility needs to be determined. Therefore, mobility management for LDM pairs is crucial for the successful broader implementation of LDM in the future wireless network.

The following section describes the usage scenario where such user IoT pairing would be needed. Both urban and rural scenario showing the usages model is presented. The focus is mainly on the IoT usages as these are the expected new inclusion in future wireless communication.

3 Use case scenario of LDM in future wireless network

Our system model focuses on heavy downlink communication for IoT and users [14]. It is widely assumed within the predecessor communication technologies that IoT communication does not require much downlink data. However, the future usage models are expected to demand more uplink and downlink data transmission for both users and IoT devices. This section aims to describe a few such future transmission scenarios where our proposed system model can be of use to support such transmission. We have considered both urban and rural scenarios for such possible heavy downlink transmission dependency for mMTC communication. These possible usages scenarios justify our downlink heavy transmission model for IoT communication.

3.1 Urban use-case scenario for IoT downlink communication

The urban areas are expected to be high devices density areas. Fig. 1 depicts a transmission scenario for the downlink communication requirements for autonomous vehicle systems and cloud-controlled drones in the future city context. Small cell or picocells are expected to adopt in urban cellular infrastructure.

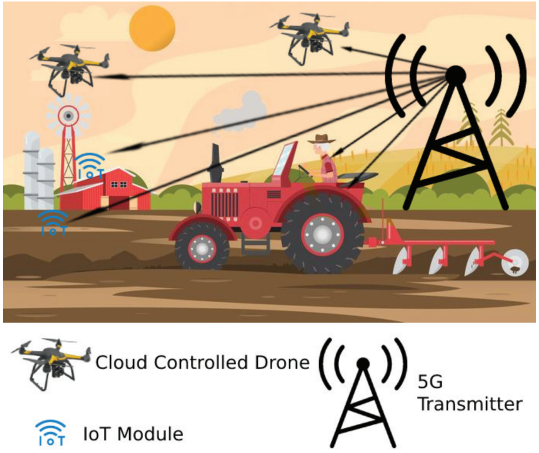

Fig. 2. Downlink transmission model for IoT devices in rural area

Hence, a transmitter is expected to take advantage of existing urban structures such as radioheads installed on the lamp-post, as shown in Fig. 1 [15]. Alongside the massive number of IoT devices attached to users, such as smartwatches and other devices, cloud control drones and autonomous vehicle systems will add to the total number of IoT users in future cities. The drones in this Fig. 1 are controlled from a central cloud location, requiring constant control information from the cloud depicting high downlink communication dependency. Autonomous vehicles also have a heavy downlink dependency as they also require continuous traffic and control information from the cloud to navigate the urban streets [16]. Most of these communications are expected to be real-time communication; hence they require ultra-reliable low latency communication [17]. As the number of users and IoT devices are expected to multiply significantly, future wireless networks need to achieve the capability to manage such a high number of connections. Due to the similarities of payload information in most of the associated machine type devices, any IoT device can be paired with a suitable user device. In this configuration, the UL layer is suitable for all IoT devices due to its robustness and lower latency.

3.2 Rural use-case scenario for IoT downlink communication

The application of IoT in the rural scenario is different from that of the urban scenario depicted in the earlier section. Many future farming and agriculture systems will be controlled and monitored by IoT sensors, and cloud-controlled drones can be useful for surveillance, as shown in Fig. 2. The drones need real-time control information as described in urban scenarios; sensors also have significant use for future rural applications, for example, to monitor water flow, assess stored food conditions, and different agriculture-related monitoring. These devices can serve multiple services based on the requirement and are expected to be self-reconfigurable upon receiving control information from the clouds. Subsequently, these devices require a heavy downlink transmission. One major change in the network configuration of rural areas is the use of cells with large coverage areas. This large cellular coverage area will make the user IoT pair more sustainable even when both are receiving devices are mobile. However, the design of LL will be more critical to the extensive coverage area and hence will be more susceptible to channel conditions. However, the slow nature of changes in rural areas makes for better channel prediction. Hence, the UL and LL can serve these IoT and user combinations in such scenarios.

A physical layer transceiver framework that adopts LDM within a standard OFDM model is described next. The model is for a two-layer LDM transmission where UL serves the IoT devices, and the LL is used to serve the user.

4 Transceiver Framework Adopting LDM

We have proposed the integration of LDM within an OFDM system as shown in Fig. 3. We are focusing on benchmarking the performance of LDM layers within an OFDM framework, and for that purpose, have not included any error-correcting code in our proposed model. Like any communication model, the system is described as per transmitter, channel and receiver.

Transmitter framework with LDM superposition The processing of both UL and LL data is done in parallel at the transmitter end, as shown in Fig. 3. Both layers can have different transmission bit rate with different Quadrature Amplitude Modulation (QAM) modulation scale M. The UL will have a lower bit rate hence a lower M, and the opposite is assumed for the LL. However, M is chosen in a way that will result in an equal number of UL and LL QAM symbols. LDM superposition is done in the next step, resulting in the same number of LDM symbols. The power of the LL symbol is reduced during the superposition process to have a smaller power portion of the total transmit power. The total transmission power is the same as any single-core transmission. Equation (1) represents the LDM superposition where $\mathbf{X(}k\mathbf{)}$ represents the LDM symbols of kth sub-carrier, g is the power ratio between layers, and $\mathbf{X_{UL}}(k)$, $\mathbf{X_{LL}}(k)$ represent UL and LL symbols of kth sub-carrier, respectively. As a result, each LDM symbol contains a UL layer symbol and a LL symbol where the total number of LDM symbols is the same as that of an OFDM system in a sub-carrier.

$$\mathbf{X}(k) = \mathbf{X_{UL}}(k) + g\,\mathbf{X_{LL}}(k). \tag{1}$$

Channel model A single traffic channel serves user-IoT paired devices with LL and UL layer data. In this analysis, we have considered the AWGN channel model. The IoT device and user come under various mobility models, and hence the channel condition will vary for both of them. However, the IoT devices are

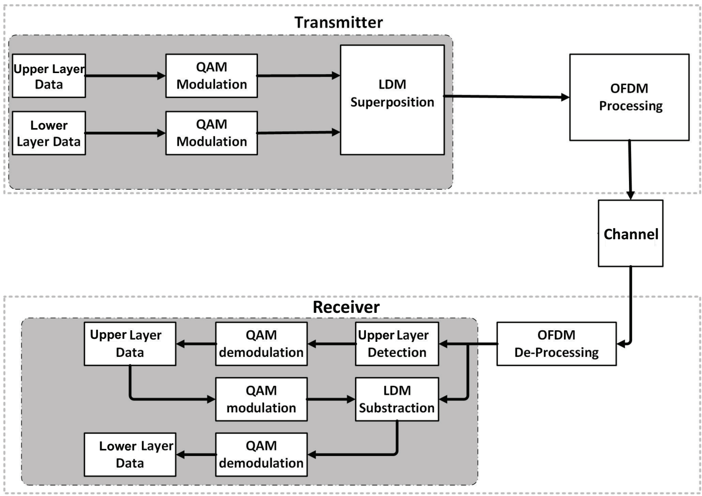

Fig. 3. OFDM transmission framework with LDM adaptation

assumed to be in poorer channel conditions due to their versatile locations and power restrictions, making them ideal recipients of UL data. The user device is more sensitive to channel conditions, but it can enjoy a higher data rate due to the properties of LL. We assume perfect channel estimation and perfect reception of control signalling at the receivers, and receivers have all the necessary information needed to detect the signal.

Receiver framework for LDM detection The LDM signal at the receiver can be expressed by

$$\mathbf{Y}(k) = \mathbf{X_{UL}}(k).\,\mathbf{H}(k) + g\,\mathbf{X_{LL}}(k).\,\mathbf{H}(k) + \mathbf{N}(k), \tag{2}$$

where $\mathbf{Y}(k)$ is the received signal of kth sub-channel, $\mathbf{H}(k)$ is the channel matrix, and $\mathbf{N}(k)$ is the added noise. The dimensions of all the parameters used in (2) are the same as the number of OFDM symbols of kth sub-carrier, which we assumed to be 64 in our simulation. The UL detection is done in a simple OFDM detection process where the LL signal from (2) is treated as added interference. Equation (3) shows the total noise and interference for the UL detection. UL detection does not require complex computing; hence this is suitable for low power IoT devices. The signal at the receiver will have the originally transmitted signal with added noise as well as channel effects and can be expressed as

$$\mathbf{N_{UL}}(k) = g\,\mathbf{X_{LL}}(k)\,.\,\mathbf{H}(k) + \mathbf{N}(k). \tag{3}$$

The detection of LL data is done in the next phase, where the detected UL data is processed the same way as it is done at the transmitter. The reconstructed UL data was then subtracted from the original received signal. Then the remaining signal is amplified and detected in that order. Equation (4) shows the subtracted signal for the LL detection.

$$\mathbf{Y_{LL}}(k) = \mathbf{X_{UL}}(k).\, \mathbf{H}(k) + g\, \mathbf{X_{LL}}(k)\,.\, \mathbf{H}(k) + \mathbf{N}(k) - \mathbf{X_{UL\ re}}(k). \quad (4)$$

Assuming a perfect UL detection with perfect channel estimation, we can derive LL signal as

$$\mathbf{Y_{LL}}(k) = g\, \mathbf{X_{LL}}(k)\,.\, \mathbf{H}(k) + \mathbf{N}(k). \quad (5)$$

The signal from (5) is amplified with a factor of $1/g$ before the detection of LL data. As we can not separate noise during this phase of detection, the noise is also amplified by the same ratio, and it makes the LL data detection more prone to channel noise power level. Successful UL detection is essential in this transmission framework for successful LL detection, so the UL needs to be reliable and robust. Moreover, the LL data detection process is more computationally intensive, so user devices require higher computation capability.

The analytical model to evaluate the UL bit error rate (BER) is developed empirically, and described in the following section. The Chanel capacity distribution and the maximum UL channel capacity is also derived.

5 Theoretical Evaluation

We analyzed the system models described in the last section to evaluate the performance of LDM in our proposed usage models. To justify the results of this analysis and have a reference point for future work, we have developed an empirical equation to examine the performance bound of the LDM UL. Due to the incorporation of LL data, the maximum UL channel capacity is bounded by the g. This capacity bound is also defined in this section.

5.1 Bit error rate of LDM upper layer

We considered the performance of LDM in an uncoded OFDM system in the AWGN channel. We have obtained the equation for symbol error rate (SER) of an uncoded QAM OFDM system from [18] as

$$SER_k^{AWGN} = 4\left(1 - \frac{1}{\sqrt{M}}\right) Q\left(\sqrt{\frac{3\,\rho_k}{M-1}}\right) - 4\left(1 - \frac{1}{\sqrt{M}}\right)^2 Q\left(\sqrt{\frac{3\,\rho_k}{M-1}}\right)^2, \quad (6)$$

where

$$Q(x) = \frac{1}{pi} \int_0^{\frac{pi}{2}} \exp\left(-\frac{x^2}{2\sin^2\theta}\right) dx \quad (7)$$

and ρ_k is the SNR of the kth symbol.

By assuming Gray coding for QAM constellation, which gives a single bit error for each symbol error, we get the relation between BER and SER as BER = SER/M. An analytical model for the BER calculation of the UL is developed from the equations above. For evaluation, no inter symbol interference is assumed. LL has lower power than the UL; therefore, the value of g is always negative in dB. We apply this setup for all the different QAMs used. We identified that the UL data rate and g follow the relation in an uncoded OFDM system as

$$g = -4\,M_c \tag{8}$$

where M_c is the QAM order for the UL. Now, the UL SNR is calculated from channel SNR as

$$\rho_{kcl} = \frac{2\,\rho_k}{-g}. \tag{9}$$

Using the values of UL SNR from (9) in (6) we calculate the SER of the UL data as

$$\begin{aligned} SER_k^{AWGN} = 4\left(1-\frac{1}{\sqrt{M}}\right) Q\left(\sqrt{\frac{6\,\rho_k}{g(1-M)}}\right) \\ - 4\left(1-\frac{1}{\sqrt{M}}\right)^2 Q\left(\sqrt{\frac{6\,\rho_k}{g(1-M)}}\right)^2 . \end{aligned} \tag{10}$$

5.2 Channel capacity distribution

The channel capacity of an AWGN channel can be written as

$$C = \log_2\left(1+\frac{P_s}{P_n}\right), \tag{11}$$

where P_s is the signal power and P_n is the noise power. This shows the dependency between channel SNR and capacity, and can be used to calculate the channel capacity for LDM layers as [10]

$$C_{UL} = \log_2\left(1+\frac{P_{UL}}{P_{LL}+P_n}\right) \tag{12}$$

and

$$C_{LL} = \log_2\left(1+\frac{P_{LL}}{P_n}\right). \tag{13}$$

As the power ratio g is known, we can evaluate the UL's maximum system capacity with a fixed value of g from

$$C_{UL} = \log_2\left(1+\frac{1}{g}\right). \tag{14}$$

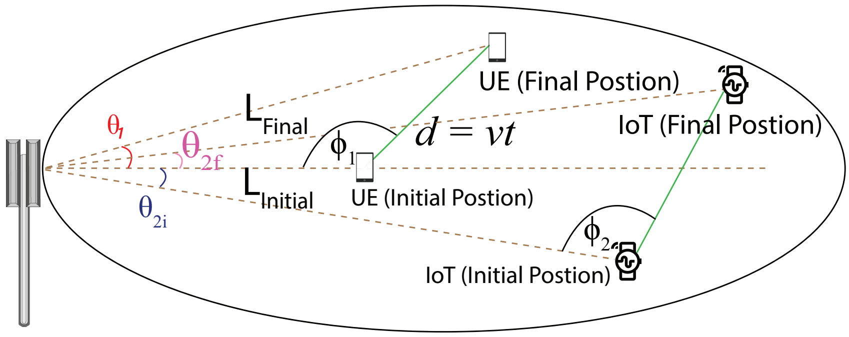

Fig. 4. IoT and user mobility in LDM pairing

The following section considers a model where both user and IoT receivers are mobile. A detailed analysis of LDM pair sustainability with mobility is presented in the next section.

6 Mobility model

We are considering both user and IoT mobility in this analysis. In ATSC 3.0, a 4k-Ultra High Definition TV or multiple enhanced HDTV services are transmitted using LL to a fixed receiver with advanced antennas [19]. The proposed model is developed to test the UL and LL layers' performance with various mobility models for users and IoT devices. Moreover, the future wireless network is expected to use advanced transmission technology such as massive MIMO to transmit configurable signals with custom power and beamwidth management. These technologies will allow the system to manage interference and frequency reuse more efficiently. However, these techniques will lower the coverage area with narrower beamwidth and lower transmission power. This smaller coverage area will be more challenging to sustain the mobile LDM pair. Ideally, we want our LDM pair to be within the coverage area for the duration of the entire data transmission to minimize the effort needed to form new IoT-user pair. Therefore, there is a trade-off between the transmission beam width and power and the optimum coverage area for a different receiver mobility group.

6.1 IoT and user mobility

As shown in Fig. 4, the IoT devices are assumed to be distributed randomly over the entire transmission, and the initial beam is directed at the user location; hence it is at a zero degree angle with the transmission beam. The IoT devices can start with any random angle θ_{2i} with transmission direction. Fig. 4 shows the mobility of IoT and user devices from an initial position to a final position. The base station (BS) is assumed to be located at position (x_b, y_b). The initial

IoT and user location is assumed to be at (x_1, y_1). Then the initial distance L_{initial} can be calculated using

$$d = \sqrt{(x_1 - x_2)^2 + (y_1 - y_2)^2}. \tag{15}$$

The transmission is assumed to be directed at the user's initial position. Therefore, the user is initially located on the x-axis, as shown in Fig.4. The distance between the user's initial position and the base station is the same as the x values of the user's initial coordinates.The initial angle between IoT device and BS θ_{2i} can be calculated as

$$\theta_{2i} = \cos^{-1}\left(\frac{l_{\text{initial}}^2 + x_1^2 - y_1^2}{2l_{\text{initial}}\, x_1}\right). \tag{16}$$

If the device moves at a random speed v for a time t to reach its final position, then the distance between IoT's initial and final position d can be written as

$$d = v\, t. \tag{17}$$

The IoT device is assumed to move at a random angle ϕ to the (x_2, t_2) after time t. Then the final position can be calculated using

$$x_2 = x_1 + d\cos(\phi), \tag{18}$$

and

$$y_2 = y_1 + d\sin(\phi). \tag{19}$$

The coordinates of BS and IoT is now known. The distance between the initial and final location of IoT and with BS can be measured using (15). At the final position, the angle between BS and IoT is taken as θ_2 as shown in Fig. 4 which can be calculated as

$$\theta_{2f} = \cos^{-1}\left(\frac{l_{\text{final}}^2 + x_2^2 - y^2}{2l_{\text{final}}\, x_2}\right). \tag{20}$$

Similarly for user device, the final angle θ_f can be calculated using the following values of user's initial and final position.

$$\theta_f = \cos^{-1}\left(\frac{l_{\text{initial}}^2 + l_{\text{final}}^2 - d^2}{2l_{\text{initial}}\, l_{\text{final}}}\right). \tag{21}$$

By assuming t_p as the power transmitted from the BS with n_p being the white noise power, h being the channel fading. Path-loss L_p can be calculated as [20]

$$L_p = 32.4 + 20\log_{10}(f_c) + 20\log_{10}(r), \tag{22}$$

where f_c is the carrier frequency in GHz, and r is the distance between transmitter and receiver in meters. Then finally, we can calculate the SNR at IoT devices from

$$\rho = \frac{t_p\, h\cos\theta}{n_p\, L_p}, \tag{23}$$

where h is the time selective fading coefficient. For L number of transmission paths, h depends on the career frequency f_c and Doppler frequency f_d. The following equation provides the relation between h and these above parameters as a function of time.

$$h(t) = \sum_{i=0}^{L-1} a_i \, e^{-j\,2\,\pi\, f_c\, \tau_i} \, e^{j\,2\,\pi\, f_d t}. \tag{24}$$

From this relation, we can calculate h from the carrier frequency f_c and the speed of the devices, which is the cause of the Doppler frequency f_d. We assume the SNR of IoT at the initial position as ρ_1. IoT data is transmitted using the UL, and LDM configuration is developed based on ρ_1 and user network conditions. As the IoT and user device moves from the initial position, the SNR condition will keep changing. The LDM pair needs to break when the minimum SNR required for the IoT devices or the user is greater than the channel SNR of either devices.

6.2 The range of IoT device's initial position

When forming LDM pair, both user and IoT devices need to be within the coverage area. As the transmission is directed towards the user, we need to sort out the boundary condition for the IoT device that will keep it within the transmission angle. To simplify, we are assuming the base station location as (0,0), we get the initial distance between BS and IoT as

$$\begin{aligned} L_{initial} &= \sqrt{(x_b - x_1)^2 + (y_b - y_1)^2} \\ &= \sqrt{x_1^2 + y_1^2}. \end{aligned} \tag{25}$$

Using (16) and (25) we can derive the following relation

$$\begin{aligned} cos(\theta_1) &= \frac{L_{initial}^2 + x_1^2 - y_1^2}{2\, L_{initial}\, x_1} \\ &= \frac{x_1^2 + y_1^2 + x_1^2 - y_1^2}{2\, L_{initial}\, x_1} \\ &= \frac{2\, x_1^2}{2\, L_{initial}\, x_1} \\ &= \frac{x_1}{L_{initial}}. \end{aligned} \tag{26}$$

For the IoT device's initial position to be within the transmission area, the maximum value of θ_1 can be $\theta_{max} =$ Beamwidth/2. For this θ_{max} angle, we can calculate the maximum value of the initial y position from a given x position using (26) and derive the following relation.

$$\begin{aligned}
\frac{cos(\theta_1)}{x_1} &= \frac{1}{L_{initial}} \\
L_{initial} &= \frac{x_1}{cos(\theta_1)} \\
x_1^2 + y_1^2 &= \frac{x_1^2}{cos^2(\theta_1)} \\
y_1^2 &= \frac{x_1^2}{cos^2(\theta_1)} - x_1^2 \\
y_1 &= \sqrt{\frac{x_1^2}{cos^2(\theta_1)} - x_1^2}. \qquad (27)
\end{aligned}$$

Equation (27) gives the maximum limit on the initial y position for IoT device for any given x value and transmission beamwidth.

6.3 Mobility model

In the proposed scenario, we have considered IoT devices attached to human usages, such as smartwatches, car sensors and similar devices. So the mobility model of these devices is similar to the human mobility model. We have considered the following three mobility models for IoT movement.

Random Way-point mobility model This mobility model represents static to downward movement in urban and rural areas. This movement model applies to non-motorised movements such as walking, running, and cycling. The speed of the users in this model is assumed to be within the range of 0 to 10 kph, and the angle is between 0 to 360 degree. The movement pattern is random both in terms of speed and direction as both can be changed randomly at any time [21]. For simplicity, we have assumed that the devices can alter their speed after every t time interval and direction after every 100 meter.

Manhattan mobility model This model refers to the urban street movement for motorised vehicles [21]. The roads are assumed to be in a grid design with the change of direction can only be multiple of 90-degree angle. We assume the block lengths to be 200 meter for this work, which means the user can change direction every 200 meter with a speed range between 10 to 40 kph.

Free-way mobility model This mobility model is for unidirectional mobility. In this model, the device keeps moving in a constant direction for the whole scenario with variable speed. We have taken this model to represent vehicle movement on the motorway. This model assumed the vehicle speed to be between 40 to 100 kph. Moreover, as the vehicle does not take turns frequently and moves

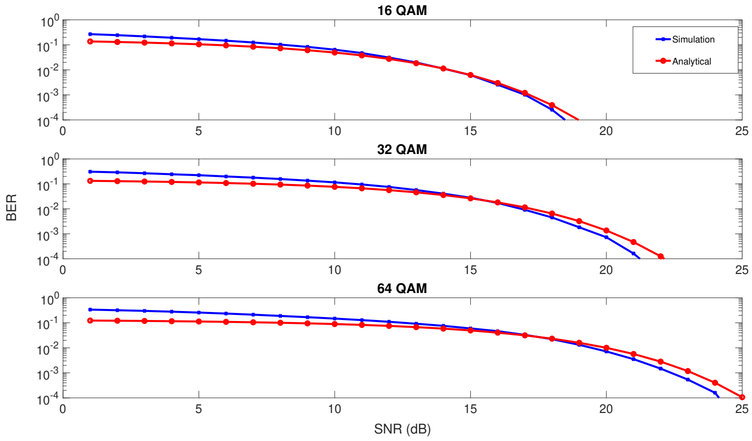

Fig. 5. Performance comparison of LDM UL between simulation and analytical results for 16, 32 and 64 QAM modulation

freely via a single road at a higher speed, we can assume their movement to be unidirectional for a more petite time frame. This model is a simple linear model where the receiver's position can be predicted.

7 Results and Analysis

We are presenting two sets of analyses to evaluate our transmission framework. In the first set, we test the performance of LDM transmission without any additional channel coding. The results show different channel SNR requirements for UL and LL data detection. Moreover, our analytical model is also verified in this analysis. In the second set we test the link sustainability of LDM pair with mobility. All our previously discussed mobility models are considered in this simulation, and the results show the feasibility of LDM for mobile receivers.

7.1 The performance of LDM in an OFDM framework

In this simulation, two independent data sets are transmitted using LDM within an OFDM framework using an AWGN channel model. The SNR values presented in the results refer to the overall channel SNR for the OFDM signal. Table 1 presents the parameter used in these simulations. The analytical model in (10) is also evaluated alongside the simulated values. The distribution of channel capacity between UL and LL is also given, which provides a clear indication of the applicability of both layers for IoT devices and users, respectively.

The performance bound of the UL layer presented in the earlier section is evaluated in Fig. 5. The BER performance follows a waterfall curve as the BER

Table 1. OFDM parameters used for LDM simulation

Parameter	Values
No. of carriers	64
Single frame size	96 bits
Total no of frame	1000
No. of pilot bits	4
Cyclic extension	16 bits

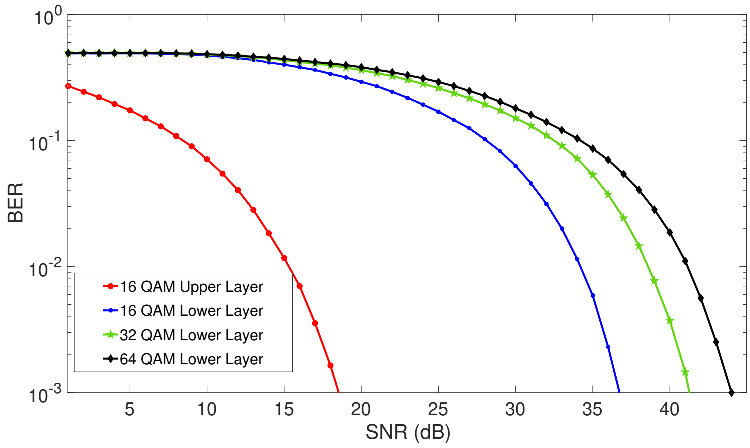

Fig. 6. BER performance of LDM LL transmission for 16, 32 and 64 QAM constellation with a fixed UL data rate

decreases with channel SNR. The SNR does not calculate the additional interference to UL data from LL data. We have tested the UL performance for different data rates, which is varied by QAM modulation index M (16, 32, and 64) and the power ratio g is selected as per (8). From the figure, we see overlapping BER performance for analytical and simulation results, which shows the correctness of our developed performance bound. This equation can be used to evaluate future works on LDM and OFDM. Another noticeable characteristic from the results is the increment of SNR values for similar BER performance as the data rate increases.

Fig. 6 compares the performance of UL and LL and evaluate their performance with our proposed IoT-user LDM usage models. The power ratio g is set fixed at -10 dB in this analysis. We simulated the system with different data rate combinations for the UL and LL. The UL data are fixed at 192 bits (16 QAM) per frame, while the LL data ranges from 192 bits (16 QAM), 240 bits (32 QAM) and 288 bits (64 QAM) per frame. The UL performance is unchanged with the different data rates of the LL. Moreover, we obtain a bit error rate of

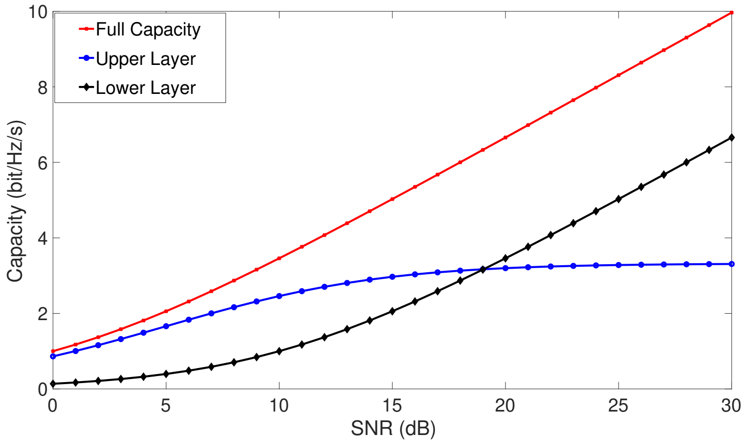

Fig. 7. Distribution of channel capacity between LDM UL and LL for fixed power ratio g

10^{-4} at around 22 dB. In [22], the authors investigated the UL performance for QPSK with a strong low-density parity-check (LDPC) coding of 4/15. They achieved the same 10^{-4} bit error rate at 7 dB. They also attained a similar LL performance for 64 QAM at 20 dB. In another work, [23] used BPSK for the UL with 1/8 Turbo coding for error correction and QPSK for LL with 1/2 turbo coding and achieved a similar performance at 1 and 15 dB, respectively. We get a similar performance of LL around 40 dB channel SNR for uncoded OFDM system. Our model requires higher SNR due to lack of error correction ability as we were focused on finding the performance of LDM itself. However, we also have around 15 dB higher SNR requirement for LL than UL, which is similar to the results found in [23]. Similar to the earlier results, higher SNR is needed to achieve similar BER performance with a higher data rate. Fig. 6 shows the channel condition required for different receivers. The receiver of the UL can be in the worse transmission area with a poor SNR, whereas the receiver of the LL needs to be in a good coverage area for successful detection. The BER performance of UL at lower SNR works well for small IoT devices as they will be distributed among different places with varying channel conditions. On the other hand, LLs need higher SNR values, as seen in Fig. 6, which is more suitable for users due to their better channel condition and data requirement.

Channel capacity distribution between the LDM data layers is explained using (11), (12) and (13). Fig. 7 shows the total channel capacity distribution between the LDM layers. The figure shows that the capacity distribution is lossless and non-linear. At lower SNR, the UL capacity is higher than that of the LL. However, it gets saturated with an increase in SNR, which can be calculated using (14) and shows the maximum UL capacity in any given LDM configuration. This distribution works well for IoT devices in our usage model as the devices are

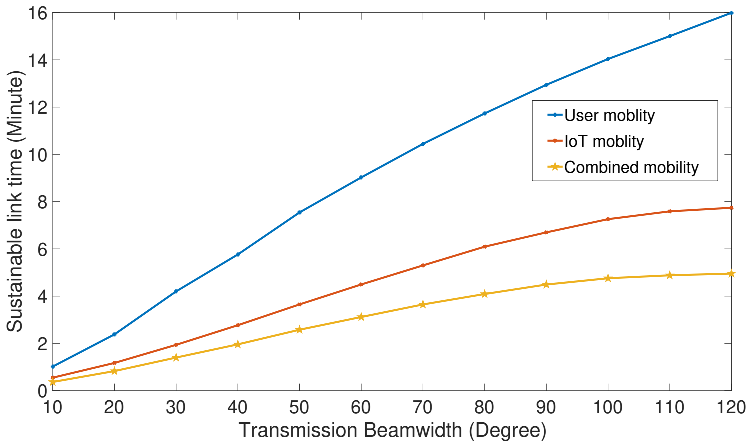

Fig. 8. Impact of the LDM pair mobility on the sustainable link time for random way-point mobility model.

assumed to be in different locations, which can cause bad channel conditions for some devices. Due to the robustness of the UL against the channel conditions, it can be used to serve all IoT devices. Moreover, the UL capacity is lower, which also fits with the IoT devices data requirements we assumed in our usage model. On the other hand, the LL has a low capacity at lower SNR. The capacity of LL increases significantly as the SNR values improve. LL has most of the available channel capacity in good channel conditions.

7.2 Receiver mobility

We have simulated the user and IoT mobility based on the earlier mobility models. The LDM pair performance is evaluated for link sustainability for a different mobility model and transmission beamwidth combination. In the first case, the user is assumed to be static while the IoT device is mobile. The x position of the IoT devices is between 0 to 500 meter and is randomly chosen in each iteration. The range of y position is calculated using the known transmission beamwidth, x and (27). In the second case similar simulation is done for the user movement, assuming that the transmission angle is set based on the user's initial position. Moreover, we simultaneously moved both IoT and the user to determine the sustainable link time in the final setup. We have combined the random way-point and Manhattan model to test the link sustainability of such mobility combination. These comparisons will help the system form LDM pairs more efficiently based on the mobility group of the receivers. Both models represent urban areas, whereas the free-way mobility model is for separate geographical areas.

In both Fig. 8 and 9, the IoT devices are moving according to the random way-point mobility model while we change the mobility model for users. In Fig. 8

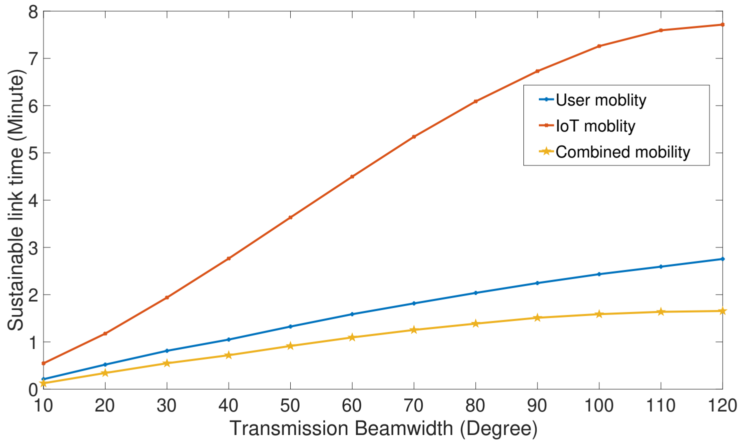

Fig. 9. Impact of the LDM pair mobility on the sustainable link time for random way-point model for IoT and Manhattan model for user.

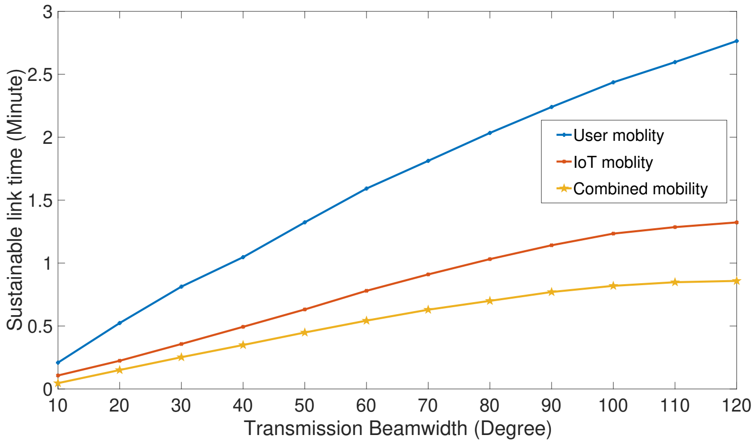

Fig. 10. Impact of the LDM pair mobility on the sustainable link time for Manhattan mobility model.

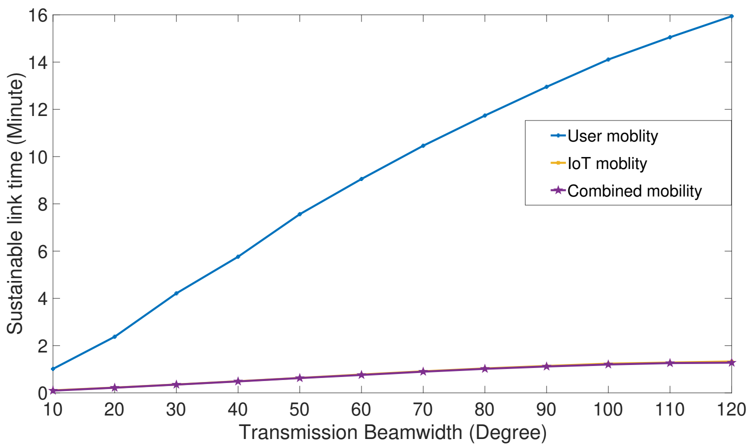

Fig. 11. Impact of the LDM pair mobility on the sustainable link time for Manhattan model for IoT and random way-point model for user.

both IoT and user devices are in the same mobility group. User mobility has less impact on pair sustainability as the transmission is directed towards the user. The IoT devices go out of the transmission area faster as there are cases when the IoT devices initial position can be at the network edge, which will break the LDM pair more quickly. The combined results follow a similar trend as IoT mobility, and as expected, the combined mobility offers a shorter sustainable link time. In Fig. 9, the user is on a higher mobility model, hence performs worse than IoT. We see a similar pattern in this case as well, where the combined mobility serves less than the user mobility. From these results, this is clear that the most efficient pairing would be IoT devices and users in the same mobility group; otherwise, the system will need to find a new device for pairing as one of the devices goes out of range.

In both Fig. 10 and 11, the Manhattan mobility model is used for IoT mobility while we used different mobility models for user mobility. In Fig. 10, again, just as in the case of the random way-point mobility model, the user stays within the transmission area for a significantly longer period. At a 120 degree transmission angle, user mobility offers almost double link sustainability time than IoT mobility. Figure. 11 on the other hand, shows similar results with one exception; unlike the other results here, the combined mobility is almost the same as IoT mobility. This behaviour is due to the gap in the link sustainability time of user and IoT mobility. As user mobility offers a much higher link sustainable time, the pair needs to be broken almost every time due to the IoT device's network condition. This pattern can help the BS monitor one of the device's conditions with higher frequency based on their mobility model, lowering the computation load at the BS with higher efficiency.

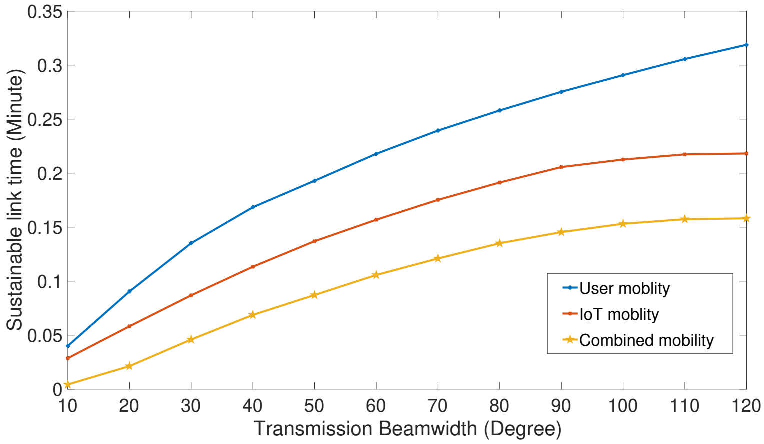

Fig. 12. Impact of the LDM pair mobility on the sustainable link time for free-way mobility model.

Table 2. Combined performance comparison for 60 degree transmission angle

Mobility model	IoT	User	Both	Ratio IoT	Ratio User
Random-Way-point	4.49	9.02	3.1	0.69	0.34
Random-Way-point Manhattan	4.49	1.58	1.09	0.24	0.68
Manhattan	0.78	1.59	0.54	0.7	0.34
Manhattan Random-Way-point	0.77	9.05	0.76	0.98	0.08
Free-Way	0.15	0.21	0.1	0.64	0.46

In Fig. 12, both IoT device and user are moving as per the freeway mobility model. Both devices are moving at a higher speed, and hence the sustainable time is much lower than the urban scenario. However, the gap in performance between IoT and user devices are lower in this scenario. In future work, other technologies such as beam-following can be applied to improve the performance in this scenario as the movement is unidirectional and predictable. Table 2 shows the comparison of link sustainability at 60 degree transmission angle for all five transmission scenarios. When both devices are in the same mobility group, IoT devices are more likely to go out of range before the user. As we can see, when the gap between user and IoT sustainability is too significant, the gap between IoT and combined mobility performance become smaller. The BS can use this knowledge of known patterns during LDM pairing and make a more efficient IoT-user LDM pair that can improve the LDM performance in future wireless networks.

8 Conclusion

The analysis presented in this chapter focuses on the performance of LDM and its sustainability when both receivers have various degrees of mobility. LDM can take advantage of the diversity of channel conditions and user requirements. An adaptive power-sharing ratio with extensive experimental measurement to use LDM UL for mMTC is developed in this work. The modelled power-sharing ratio has been explored to derive an analytical model that defines the LDM UL performance bound. The proposed analytical model has been shown to be robust for any order of modulation size, which justifies the LDM UL's feasibility for downlink communications for the future wireless network in certain downlink-heavy use cases. In this chapter, we have considered three mobility models to represent the movement of both IoT devices and users. In each case, the transmission direction is set up based on the initial user location; hence the user has a more manoeuvrable distance in all directions before it goes out of the coverage area. In contrast, the IoT devices are positioned randomly on the total coverage area, creating a scenario where IoT mobility plays a more dominant role in the sustainability of the LDM pair. The simulation results show the possibility of LDM in our proposed scenario. Future work on this area may consider machine learning to improve the accuracy of LDM pairing based on the mobility model and position of the user and IoT devices.

References

1. G. Wunder, P. Jung, M. Kasparick, T. Wild, F. Schaich, Y. Chen, S. Ten Brink, I. Gaspar, N. Michailow, A. Festag *et al.*, "5GNOW: non-orthogonal, asynchronous waveforms for future mobile applications." *IEEE Communications Magazine*, vol. 52, no. 2, pp. 97–105, 2014.
2. L. Dai, B. Wang, Y. Yuan, S. Han, I. Chih-Lin, and Z. Wang, "Non-orthogonal multiple access for 5G: solutions, challenges, opportunities, and future research trends," *IEEE Communications Magazine*, vol. 53, no. 9, pp. 74–81, 2015.
3. J. P. Lemayian and J. M. Hamamreh, "Recurrent neural network-based channel prediction in mMIMO for enhanced performance in future wireless communication," in *2020 International Conference on UK-China Emerging Technologies (UCET)*. IEEE, 2020, pp. 1–4.
4. L. Zhang, W. Li, Y. Wu, X. Wang, S.-I. Park, H. M. Kim, J.-Y. Lee, P. Angueira, and J. Montalban, "Layered-division-multiplexing: Theory and practice," *IEEE Transactions on Broadcasting*, vol. 62, no. 1, pp. 216–232, 2016.
5. S. I. Park, J.-Y. Lee, S. Myoung, L. Zhang, Y. Wu, J. Montalbán, S. Kwon, B.-M. Lim, P. Angueira, H. M. Kim *et al.*, "Low complexity layered division multiplexing for ATSC 3.0," *IEEE Transactions on broadcasting*, vol. 62, no. 1, pp. 233–243, 2016.
6. Y. Wu, B. Rong, K. Salehian, and G. Gagnon, "Cloud transmission: A new spectrum-reuse friendly digital terrestrial broadcasting transmission system," *IEEE Transactions on Broadcasting*, vol. 58, no. 3, pp. 329–337, 2012.
7. M. Earnshaw, K. Shelby, H. Lee, Y. Oh, and M. Simon, "Physical layer framing for ATSC 3.0," *IEEE Transactions on Broadcasting*, vol. 62, no. 1, pp. 263–270, 2016.

8. D. Gómez-Barquero and O. Simeone, “LDM versus FDM/TDM for unequal error protection in terrestrial broadcasting systems: An information-theoretic view,” *IEEE Transactions on Broadcasting*, vol. 61, no. 4, pp. 571–579, 2015.
9. H. Kim, J. Kim, S.-I. Park, J.-y. Lee, S. Kwon, and N. Hur, “Capacity analysis and improvement of ldm-based Multiple-PLP configurations in ATSC 3.0,” *IEEE Transactions on Broadcasting*, 2021.
10. L. Zhang, Y. Wu, W. Li, H. M. Kim, S.-I. Park, P. Angueira, J. Montalban, and M. Velez, “Channel capacity distribution of layer-division-multiplexing system for next generation digital broadcasting transmission,” in *2014 IEEE International Symposium on Broadband Multimedia Systems and Broadcasting*. IEEE, 2014, pp. 1–6.
11. L. Zhang, Y. Wu, W. Li, K. Salehian, S. Lafleche, X. Wang, S. I. Park, H. M. Kim, J.-y. Lee, N. Hur *et al.*, “Layered-division multiplexing: An enabling technology for multicast/broadcast service delivery in 5G,” *IEEE Communications Magazine*, vol. 56, no. 3, pp. 82–90, 2018.
12. L. Zhang, W. Li, Y. Wu, Y. Xue, E. Sousa, S.-I. Park, J.-Y. Lee, N. Hur, and H.-M. Kim, “Using non-orthogonal multiplexing in 5G-MBMS to achieve broadband-broadcast convergence with high spectral efficiency,” *IEEE Transactions on Broadcasting*, 2020.
13. E. Iradier, J. Montalban, L. Fanari, P. Angueira, L. Zhang, Y. Wu, and W. Li, “Using NOMA for enabling broadcast/unicast convergence in 5G networks,” *IEEE Transactions on Broadcasting*, 2020.
14. M. S. Islam, M. Patwary, R. Tait, and E. Peytchev, “Layer division multiplexing for 5G DL transmission within ultra-dense heterogeneous networks,” in *2020 IEEE 91st Vehicular Technology Conference (VTC2020-Spring)*. IEEE, 2020, pp. 1–7.
15. M. Patwary, S. K. Sharma, S. Chatzinotas, Y. Chen, M. Abdel-Maguid, R. Abd-Alhameed, J. Noras, and B. Ottersten, “Universal intelligent small cell (UnISCell) for next generation cellular networks,” *Digital Communications and Networks*, vol. 2, no. 4, pp. 167–174, 2016.
16. S. Liu, L. Liu, J. Tang, B. Yu, Y. Wang, and W. Shi, “Edge computing for autonomous driving: Opportunities and challenges,” *Proceedings of the IEEE*, vol. 107, no. 8, pp. 1697–1716, 2019.
17. H. Wang, B. Kim, J. Xie, and Z. Han, “E-auto: A communication scheme for connected vehicles with edge-assisted autonomous driving,” in *ICC 2019-2019 IEEE International Conference on Communications (ICC)*. IEEE, 2019, pp. 1–6.
18. M. Roy and H. Jamadagni, “Performance analysis of MQAM-OFDM based WLAN in presence of zigbee interference in AWGN and rayleigh fading channel,” in *2009 Sixth International Conference on Information Technology: New Generations*. IEEE, 2009, pp. 1178–1183.
19. L. Zhang, W. Li, Y. Wu, K. Salehian, S. Laflèche, Z. Hong, S.-I. Park, H. M. Kim, J.-Y. Lee, N. Hur *et al.*, “Using layered-division-multiplexing to deliver multi-layer mobile services in ATSC 3.0,” *IEEE Transactions on Broadcasting*, vol. 65, no. 1, pp. 40–52, 2018.
20. F. Khan, Z. Pi, and S. Rajagopal, “Millimeter-wave mobile broadband with large scale spatial processing for 5G mobile communication,” in *2012 50th annual allerton conference on communication, control, and computing (Allerton)*. IEEE, 2012, pp. 1517–1523.
21. R. Kumar and M. Dave, “Mobility models and their affect on data aggregation and dissemination in vehicular networks,” *Wireless personal communications*, vol. 79, no. 3, pp. 2237–2269, 2014.

22. E. Garro, J. J. Giménez, D. Gómez-Barquero, and S.-I. Park, "Performance evaluation of layer division multiplexing (LDM) combined with time frequency slicing (TFS)," in *2015 IEEE International Symposium on Broadband Multimedia Systems and Broadcasting*. IEEE, 2015, pp. 1–5.
23. E. Arruti, M. Mendicute, and M. Barrenechea, "QoS in industrial wireless networks using LDM," in *2017 IEEE International Workshop of Electronics, Control, Measurement, Signals and their Application to Mechatronics (ECMSM)*. IEEE, 2017, pp. 1–6.